BIOCHEMISTRY
including biophysical chemistry & molecular biology

Article

pubs.acs.org/biochemistry

Identification, Tissue Distribution, and Molecular Modeling of Novel Human Isoforms of the Key Enzyme in Sialic Acid Synthesis, UDP-GlcNAc 2-Epimerase/ManNAc Kinase

Tal Yardeni,[†,‡] Tsering Choekyi,[§] Katherine Jacobs,[†] Carla Ciccone,[†] Katherine Patzel,[†] Yair Anikster,[‡] William A. Gahl,[†] Natalya Kurochkina,[§] and Marjan Huizing*[,†]

[†]Medical Genetics Branch, National Human Genome Research Institute, National Institutes of Health, Bethesda, Maryland 20892, United States

[‡]Sackler Faculty of Medicine, Tel Aviv University, Tel Aviv 69978, Israel

[§]The School of Theoretical Modeling, Chevy Chase, Maryland 20825, United States

Supporting Information

ABSTRACT: UDP-GlcNAc 2-epimerase/ManNAc kinase (GNE) catalyzes the first two committed steps in sialic acid synthesis. In addition to the three previously described human GNE isoforms (hGNE1−hGNE3), our database and polymerase chain reaction analysis yielded five additional human isoforms (hGNE4−hGNE8). hGNE1 is the ubiquitously expressed major isoform, while the hGNE2−hGNE8 isoforms are differentially expressed and may act as tissue-specific regulators of sialylation. hGNE2 and hGNE7 display a 31-residue N-terminal extension compared to hGNE1. On the basis of similarities to kinases and helicases, this extension does not seem to hinder the epimerase enzymatic active site. hGNE3 and hGNE8 contain a 55-residue N-terminal deletion and a 50-residue N-terminal extension compared to hGNE1. The size and secondary structures of these fragments are similar, and modeling predicted that these modifications do not affect the overall fold compared to that of hGNE1. However, the epimerase enzymatic activity of GNE3 and GNE8 is likely absent, because the deleted fragment contains important substrate binding residues in homologous bacterial epimerases. hGNE5−hGNE8 have a 53-residue deletion, which was assigned a role in substrate (UDP-GlcNAc) binding. Deletion of this fragment likely eliminates epimerase enzymatic activity. Our findings imply that GNE is subject to evolutionary mechanisms to improve cellular functions, without increasing the number of genes. Our expression and modeling data contribute to elucidation of the complex functional and regulatory mechanisms of human GNE and may contribute to further elucidating the pathology and treatment strategies of the human GNE-opathies sialuria and hereditary inclusion body myopathy.

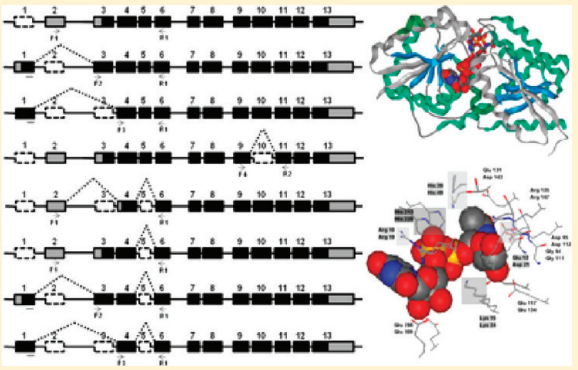

The bifunctional enzyme uridine diphosphate (UDP)-*N*-acetylglucosamine (GlcNAc) 2-epimerase/*N*-acetylmannosamine (ManNAc) kinase (GNE), encoded by the *GNE* gene, catalyzes the first two committed, rate-limiting steps in the biosynthesis of *N*-acetylneuraminic acid (Neu5Ac).[1,2] Neu5Ac is the most abundant mammalian sialic acid and the precursor of most naturally existing sialic acids.[3] Sialic acids are negatively charged, terminal residues on glycoconjugates and assist in many cellular functions, including cell−cell interactions, proliferation, and viral or bacterial infections.[3,4] The GNE enzyme consists of two enzymatic domains. The N-terminal domain is responsible for UDP-GlcNAc epimerase function, whereas the C-terminal domain is responsible for ManNAc kinase activity. In mammals, the end product of sialic acid synthesis, CMP-Neu5Ac, feedback-inhibits the UDP-GlcNAc 2-epimerase activity of GNE by binding to its allosteric site.[5]

Two distinct human disorders, sialuria (OMIM 269921) and hereditary inclusion body myopathy (HIBM; OMIM 600737), are associated with predominantly missense mutations in *GNE*. Sialuria is an autosomal dominant disorder characterized by coarse facies, variable developmental delay, hepatomegaly, and recurrent infections. To date, only seven sialuria patients have been described worldwide. All patients have a heterozygous missense mutation affecting the allosteric site of *GNE*, leading to loss of feedback inhibition of GNE epimerase activity by CMP-Neu5Ac, resulting in excessive sialic acid production.[6,7] HIBM and its allelic Japanese disorder, distal myopathy with rimmed vacuoles, or DMRV (OMIM 605820), are autosomal recessive neuromuscular disorders of adult onset, characterized by slowly progressive muscle weakness and atrophy. More than

Received: July 8, 2011
Revised: September 9, 2011
Published: September 12, 2011

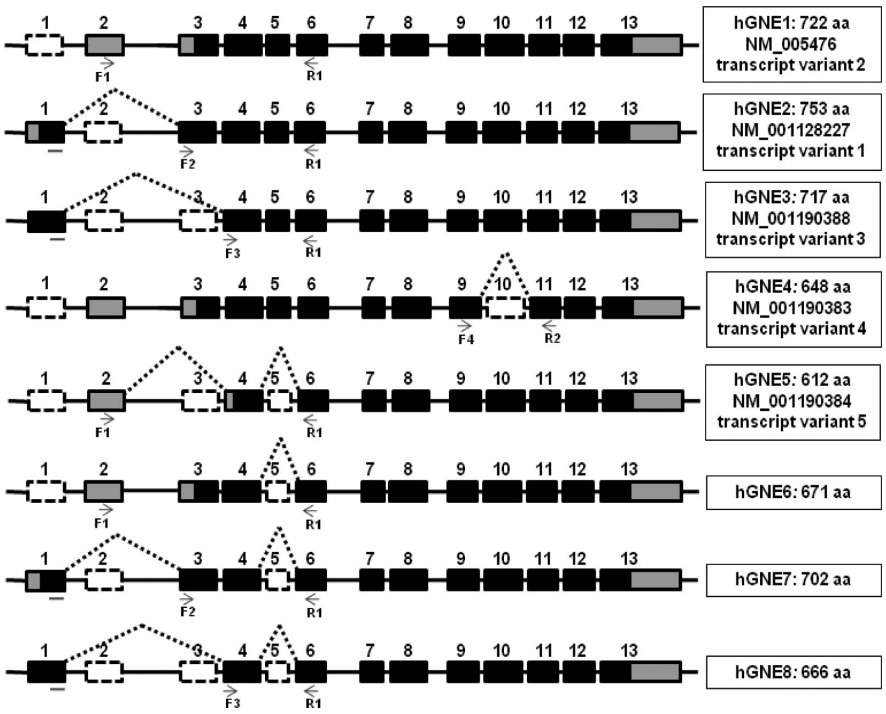

Figure 1. Eight predicted human *GNE* transcripts. Exon (boxes)−intron (lines) structures of the eight predicted human *GNE* mRNA transcripts encoding eight predicted GNE isoforms (hGNE1−hGNE8). GenBank accession numbers (when available) and the predicted number of translated amino acids (aa) are indicated. Black boxes represent the open reading frames, gray boxes the untranslated mRNA regions, and white dotted line boxes the skipped exons of each transcript. Primer locations for transcript-specific PCR amplifications (Figure 2A) are indicated as arrowed lines below each isoform. Note that forward primers F2 and F3 are localized across exon−exon boundaries.

500 HIBM/DMRV patients exist worldwide, harboring more than 60 *GNE* mutations. HIBM/DMRV patients have recessive (predominantly missense) mutations in either enzymatic domain of *GNE*, leading to decreased enzyme activity and, presumably, a decreased level of sialic acid production.[2,8,9] Whether hyposialylation is the main cause of the neuromuscular symptoms in HIBM/DMRV patients remains unknown.

In prokaryotes, GNE epimerase and kinase functions are conducted by two separate enzymes, and prokaryotic 2-epimerases have no allosteric feedback inhibition. In mammals, a bifunctional enzyme might have evolved by gene fusion of the two independent enzymes responsible for epimerase/kinase activity. Similarities between mammalian GNE N-terminal regions with prokaryotic UDP-GlcNAc 2-epimerases and mammalian GNE C-terminal regions with members of the sugar kinase superfamily previously assisted in the identification of characteristic motifs of the GNE epimerase and kinase enzymatic domains.[10,11] Bacterial 2-epimerases are allosterically regulated by their substrate, UDP-GlcNAc. A structural basis for allosteric activation was demonstrated by a crystallographic analysis of the *Bacillus subtilis* 2-epimerase in complex with the reaction intermediate UDP.[12] In addition, the crystallographic structures of the *Escherichia coli* GNE enzyme unbound and in complex with UDP-*N*-acetylglucosamine (PDB entries 1f6d and 1vgv, respectively) and the *Vibrio cholera* (PDB entry 1dzc) and *Bacillus anthracis* (PDB entry 3beo) enzymes in complex with UDP-*N*-acetylglucosamine were determined. The similarity of the N-terminal domain of the *Homo sapiens* GNE to *V. cholera* (27% homologous), *E. coli* (20% homologous), and *B. anthracis* (18% homologous) 2-epimerases was used to model its three-dimensional structure. In previous studies, structural elements and important ATP, ADP, Mg^{2+}, and substrate-binding amino acids were assigned on the basis of these similarities.[10,11] The N-terminal epimerase domain of the human GNE enzyme contains two α/β-domains (domains I and II) that form a cleft at the domain interface harboring the active site. The topology of both domains is similar to the Rossmann dinucleotide binding fold.[13] Rossmann fold domains are conserved among mammalian and bacterial 2-epimerases. The human N-terminal GNE epimerase domain has a seven-stranded parallel β-sheet sandwiched between a total of seven α-helices. The C-terminus of the GNE epimerase domain contains a six-stranded β-sheet surrounded by a total of seven α-helices.[11] Other carriers of the Rossmann fold, including glycosyltransferases and the epimerase domains of 2-epimerases, have similar N-terminal and C-terminal domains.[14,15] The crystallographic structure of the ManNAc kinase domain of human GNE was determined at 2.84 Å resolution (PDB entry 3eo3).[16] Residues 409−431 of the mammalian GNE ManNAc kinase domain showed similarities with the phosphate 1 motif of the ATP-binding domain of eukaryotic hexokinases.[10] Similar to hexokinases,[17] mammalian GNE ManNAc kinase contains a five-stranded β-sheet, β3-β2-β1-β4-β5, with β2 being antiparallel to four other parallel strands with a pair of parallel α-helices located on each side of the β-sheet (domain I). Another five-stranded β-sheet, β8-β7-β6-β9-β1, with β7 being antiparallel to four other parallel strands, is surrounded by a pair of parallel α-helices on each side (domain II). The structure of two similar domains involved in ATP binding is a common feature of the ASKHA (acetate and sugar kinase/Hsp70/actin) superfamily, described in detail for the bacterial poly(P)/ATP-glucomannokinase.[18,19]

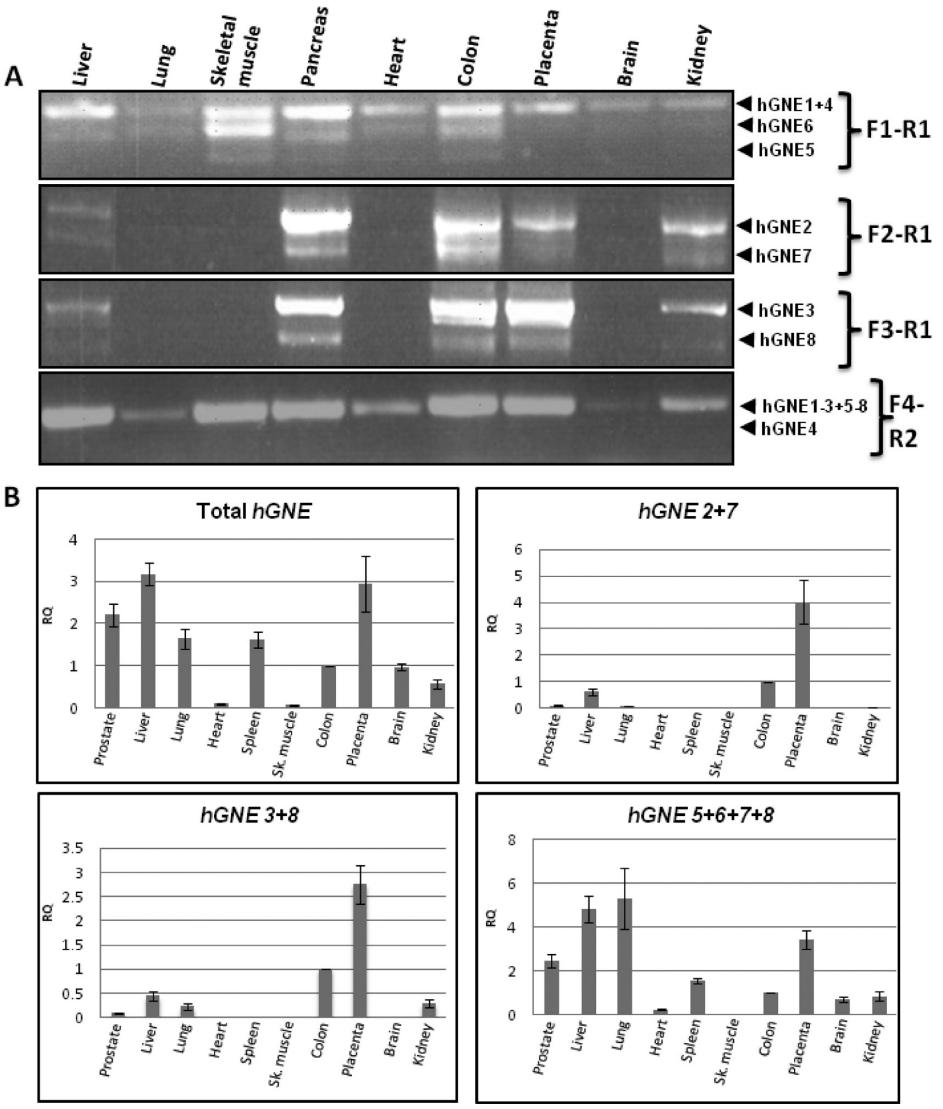

Figure 2. Tissue expression of the eight human *GNE* transcripts. (A) PCR amplification of tissue-specific cDNA from selected human tissues. Primers used for amplification and amplified isoform transcripts are indicated. (B) qPCR results of isoform-specific *hGNE* mRNA expression in a variety of human tissues. Transcript-specific TaqMan primer-probe assays were used (see Table S2 of the Supporting Information), as indicated above each panel. Displayed values represent the relative quantification (RQ) normalized to *GAPDH* with expression in colon set to 1 for each TaqMan probe. Total *hGNE* (top left panel) illustrates all *hGNE* isoforms combined (the TaqMan probe was located in the *hGNE* C-terminal part, common to all isoforms). Results are summarized in Table 1.

Recently, different human *GNE* mRNA splice variants and three predicted translated proteins, hGNE1, hGNE2, and hGNE3, were described.[20,21] Subsequently, two different mouse *Gne* mRNA splice variants were described, *Gne1* and *Gne2*, together with their expression in selected tissues.[22] In this study, we identify additional human isoforms hGNE4−hGNE8 and demonstrate expression of hGNE isoform transcripts in a wide variety of tissues. The role these isoforms play in GNE regulation or GNE-related disease pathology is unknown. On the basis of our previous modeling results with the hGNE1 isoform,[11] we now analyze and compare the structural features, with respect to catalytic activity, ligand binding, and allosteric regulation, of all eight human GNE isoforms.

EXPERIMENTAL PROCEDURES

Bioinformatics. For nucleotide sequence homology searches, National Center for Biotechnology Information (NCBI) BLAST searches were employed (http://blast.ncbi.nlm.nih.gov/Blast.cgi), as well as the Blat searches provided by the University of California at Santa Cruz (UCSC) genome browser (http://genome.ucsc.edu/cgi-bin/hgBlat). For identification of GNE homologous protein structures, sequences were retrieved from GenBank (http://www.ncbi.nlm.nih.gov/genbank/), including the human GNE1 isoform, hGNE1 (GenBank accession number NM_005476), hGNE2 (NM_001128227), hGNE3 (NM_001190388), hGNE4 (NM_001190383), and hGNE5 (NM_001190384). Atomic coordinates of proteins determined by X-ray crystallography were extracted from the Brookhaven Protein Data Bank.[23] Protein sequences were aligned using the BLAST procedure. For a cutoff of homology, an expected threshold *E* value of 0.1 was used. This value is the statistical significance threshold for reporting matches against database sequences and is comparable with a *P* value. Matches of 50 or more proteins were made. These sequence alignments were combined with structural alignments to identify structurally identical residues

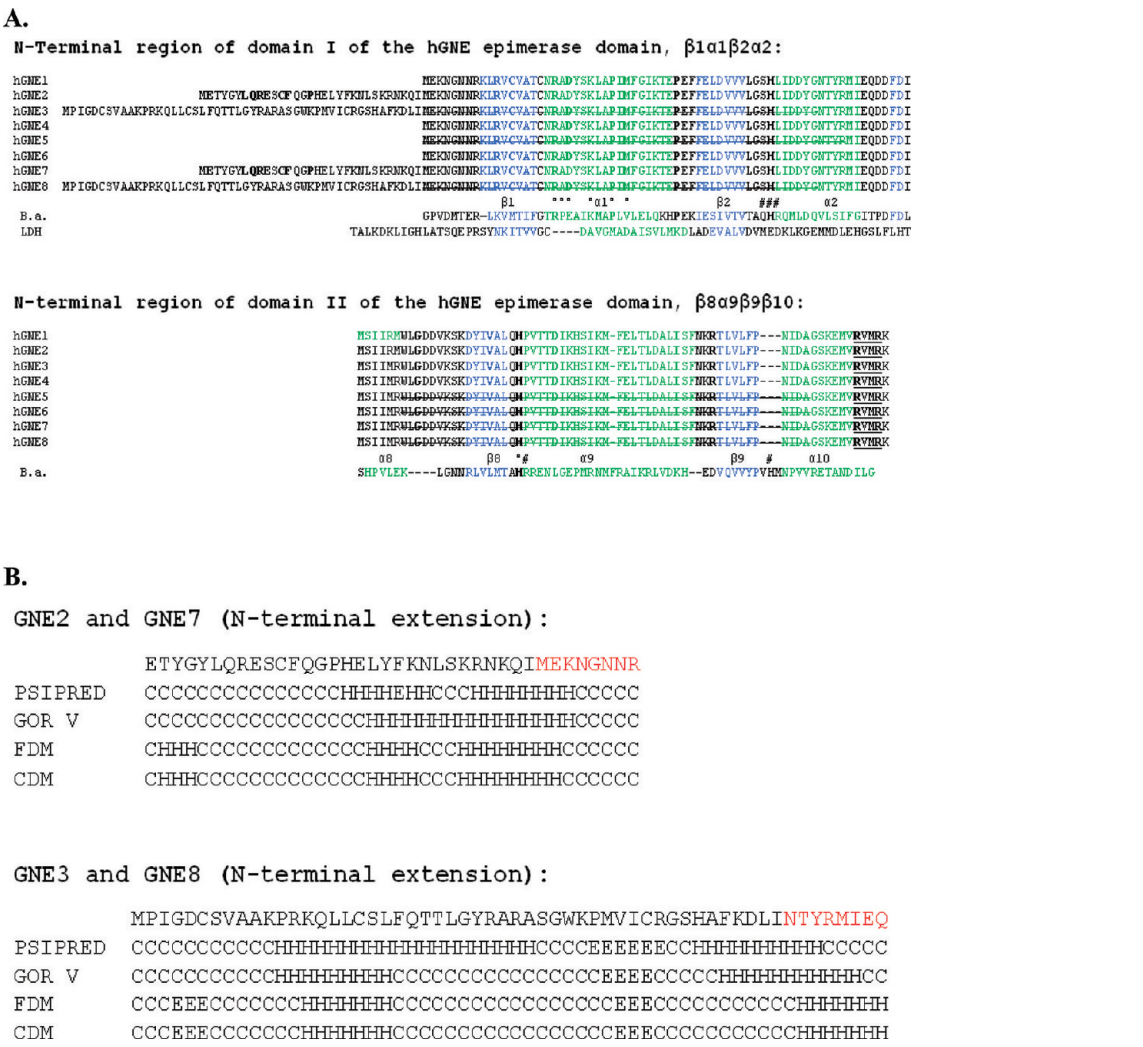

Figure 3. Sequence alignments of the human GNE isoforms. (A) Sequence alignments of the hGNE1−hGNE8 isoforms, *B. anthracis* 2-epimerase (B.a.), and *Squalus acanthias* lactate dehydrogenase (LDH). Two fragments are shown: the N-terminal region of domain I of the hGNE epimerase domain, β1-α1-β2-α2 (top), and the N-terminal region of domain II of the hGNE epimerase domain, β8-α9-β9-α10 (bottom). Strikethrough denotes amino acids deleted compared to the hGNE1 isoform: green for α-helices, blue for β-sheets, bold for amino acids that form an active site in the *B. anthracis* 2-epimerase and a putative active site in the human GNE isoforms, number signs for the allosteric site in *B. anthracis* 2-epimerase, and degree signs for glucose binding residues in *B. anthracis* 2-epimerase. (B) Secondary structure predictions (PSIPRED, GOR V, FDM, and CDM) for the N-terminal 31-residue extension of the hGNE2 and hGNE7 isoforms and the 50-residue extension of the hGNE3 and hGNE8 isoforms: C for coil, H for α-helices, E for β-strands, black for novel N-terminal extensions, and red for overlap with hGNE1 amino acids.

responsible for similar enzymatic functions. Sequences of the additional N-terminal fragments of hGNE2 and hGNE7 (Table 2) and hGNE3 and hGNE8 (Table 3) were compared with sequences of proteins (and their homologues) whose structures are known and have been deposited in the Protein Data Bank.

RNA and cDNA. Tissue-specific RNA was purchased from Clontech (human Total RNA Master Panels). cDNA was created from all RNA using a high-capacity RNA-to-cDNA reverse transcription kit (Applied Biosystems). Human multiple-tissue cDNA panels (MTC panels I and II, human fetal MTC) were purchased from Clontech Laboratories.

Transcript-Specific PCR. Primers were designed for transcript-specific PCR amplification of predicted human *GNE* splice variants (Figures 1 and 2 and Table S1 of the Supporting Information). All PCRs were performed with HotStarTaq polymerase, according to the manufacturer's instructions (Qiagen). PCR products were separated by agarose gel electrophoresis, and selected bands were excised (QIAquick Gel Extraction Kit, Qiagen) and directly sequenced using BigDye Terminator version 3.1 chemistry and an ABI 3130xl genetic analyzer (Applied Biosystems).

Quantitative Real-Time PCR. TaqMan primers and probes were ordered as premanufactured assays on demand [human *GNE* assay Hs01103402_m1 (exon 8−9)] or custom designed for splice variant-specific sequences using the ABI Assay-by-Design service (Table S2 of the Supporting Information) (Applied Biosystems). The housekeeping gene *GAPDH* [glyceraldehyde-3-phosphate dehydrogenase (Hs99999905_m1)] was used as internal control gene. All quantitative real-time PCR (qPCR) reactions and subsequent analyses were performed on an ABI PRISM 7900 HT Sequence Detection System (Applied Biosystems). The prerun thermal cycling conditions were as follows: 10 min at 95 °C to activate the *Taq*DNA polymerase, followed by 40 cycles of 95 °C for 15 s and 60 °C annealing/extension for 1 min. Each experiment was performed in triplicate. Within each experiment, reactions

were run in triplicate. Relative gene expression levels were determined by the comparative threshold cycle method (ddCt).[24]

Modeling of the Human GNE Isoforms. Secondary structure predictions for the 31-residue N-terminal extension of the hGNE2 and hGNE7 isoforms and the 50-residue N-terminal extension of the hGNE3 and hGNE8 isoforms were performed by four methods: GOR V (Garnier–Osguthorpe–Robson),[25,26] FDM (Fragment Database Mining),[27] CDM (Consensus Data Mining),[28] and PSIPRED (Protein Structure Initiative Prediction).[29] These extensions were aligned with fragments bearing similarities in amino acid sequence and assisted in determining three-dimensional structure (Figure 3B and Tables 2 and 3). Two sets of GNE epimerase domain deletions (either in GNE epimerase domain I involving isoforms hGNE3, hGNE5, and hGNE8 or in GNE epimerase domain II involving isoforms hGNE5–hGNE8) were analyzed with respect to the presence of important catalytic residues and residues involved in ligand binding and allosteric regulation.

RESULTS

Human GNE Isoforms. The human *GNE* gene (*hGNE*) consists of 13 exons, which were previously numbered exons A1, 1–12.[20] In this work, we introduce the more logical and useful numbering of *hGNE* exons 1–13 (Figure 1), a universal numbering also used by GenBank for the longest splice form of the *hGNE* gene (NM_001128227).

Three *GNE* mRNA splice variants were previously described, resulting from alternative splicing of 5′ exons 1–3,[20,21] creating three protein open reading frames, i.e., hGNE1–hGNE3, respectively (Figure 1).

hGNE1 (GenBank accession number NM_005476) is the isoform described in all previous biochemical and mutation analysis studies;[2,30,31] it encodes 722 amino acids with its translation start codon in exon 3, considered nucleotide 1 in this study and previous *GNE* mutation reports. Isoform hGNE2 (NM_001128227) has a 31-amino acid extension at the N-terminus, yielding a 753-amino acid protein with its translation start codon in exon 1 at nucleotide −93 (Figure 1). hGNE3 (NM_001190388) is extended and deleted compared to hGNE1; it has 717 amino acids with its start codon in exon 1 at nucleotide −191 (Figure 1). Note that the start codons in exon 1 for hGNE2 and hGNE3 are at different positions.[21,22] Bioinformatic database searches revealed two additional *hGNE* transcript variants, encoding hGNE4 (NM_001190383) and hGNE5 (NM_001190384), skipping the in-frame exons 10 and 5, respectively.

Tissue-specific PCR amplification (Figure 1 and Table S1 of the Supporting Information) of human cDNA tissue panels revealed hGNE1 encoding transcript expression in all tissues tested (Figure 2A and Table 1). Transcripts encoding isoforms hGNE2 and hGNE3 were expressed in the same pattern in a subset of tissues. These hGNE1–hGNE3 expression results resembled previous data,[21] with two exceptions. In brain, we found only mRNA transcripts encoding hGNE1, and not hGNE2 or hGNE3; GNE2 was previously shown to be expressed in brain. In pancreas, we found expression of hGNE1–hGNE3 transcripts; hGNE3 expression was not previously reported in pancreas.

Even though a transcript encoding isoform hGNE4 is listed in GenBank (NM_001190384), we were unable to detect expression of this transcript in the tested tissues (Figure 2A). The transcript encoding hGNE5 was minimally expressed in a subset of tissues (Figure 2A). Verification of the splice variant transcripts for hGNE4 and hGNE5 revealed three additional novel splice transcripts (Figures 1 and 2) whose protein products we named hGNE6–hGNE8. The hGNE6-encoded transcript is expressed in all tissues, similar to hGNE1. Likewise, transcripts for hGNE7 and hGNE8 followed the same expression pattern as those for hGNE2 and hGNE3 (Figures 1 and 2 and Table 1).

Table 1. *GNE* Isoform Expression in Human Tissues[a]

	hGNE1	hGNE2	hGNE3	hGNE6	hGNE7	hGNE8
liver	+	+	+	+	+	+
spleen	+	−	−	+	−	−
leukocyte	+	−	−	+	−	−
lung	+	+	+	+	+	+
skeletal muscle	+	−	−	+	−	−
pancreas	+	+	+	+	+	+
ovary	+	−	−	+	−	−
heart	+	−	−	+	−	−
thymus	+	−	−	+	−	−
colon	+	+	+	+	+	+
placenta	+	+	+	+	+	+
small intestine	+	−	−	+	−	−
prostate	+	−	−	+	−	−
kidney	+	+	+	+	+	+
brain	+	−	−	+	−	−
testis	+	−	−	+	−	−
salivary gland	+	+	+	+	+	+
trachea	+	+	+	+	+	+
adrenal	+	−	−	+	−	−
thyroid	+	+	+	+	+	+
uterus	+	+	+	+	+	+
fibroblast	+	−	−	+	−	−

[a]hGNE4 was not detected in the tested human tissues. No hGNE5-specific TaqMan assay could be designed. hGNE5-specific amplification could be detected only by conventional PCR [with very low levels of expression in selected tissues (see Figure 2A)]. Legend: +, expressed; −, not expressed; bold tissues, tissues that express all tested hGNE isoform transcripts.

We then quantified *hGNE* expression levels by qPCR in 10 selected human tissues with isoform-specific TaqMan primer-probe sets (Figure 2B, Table 1, and Table S2 of the Supporting Information). Expression of total *hGNE* mRNA differed among tissues, with the highest levels of expression in placenta and liver. The transcripts encoding isoforms hGNE2–hGNE8 showed decreased levels of expression compared to that of the hGNE1 transcript, were not expressed in some tissues (Figure 2B and Table 1), and exhibited a quantitative distribution pattern similar to that of the hGNE1 transcript in other tissues (i.e., liver, lung, and placenta).

Modeling of hGNE Isoforms. Comparison of isoforms hGNE1–hGNE8 showed that the GNE epimerase encoding domain (amino acids 1–378) exhibits differences among all isoforms, while only one isoform, hGNE4, showed differences in the kinase encoding domain (amino acids 410–722).[10,32] Because we were unable to detect hGNE4 coding mRNA transcripts in tested tissues (Figure 2A) and further analysis showed that this variant was submitted as a mutation identified in a distal myopathy with rimmed vacuoles (DMRV) patient (GenBank accession number EU093084) instead of a novel

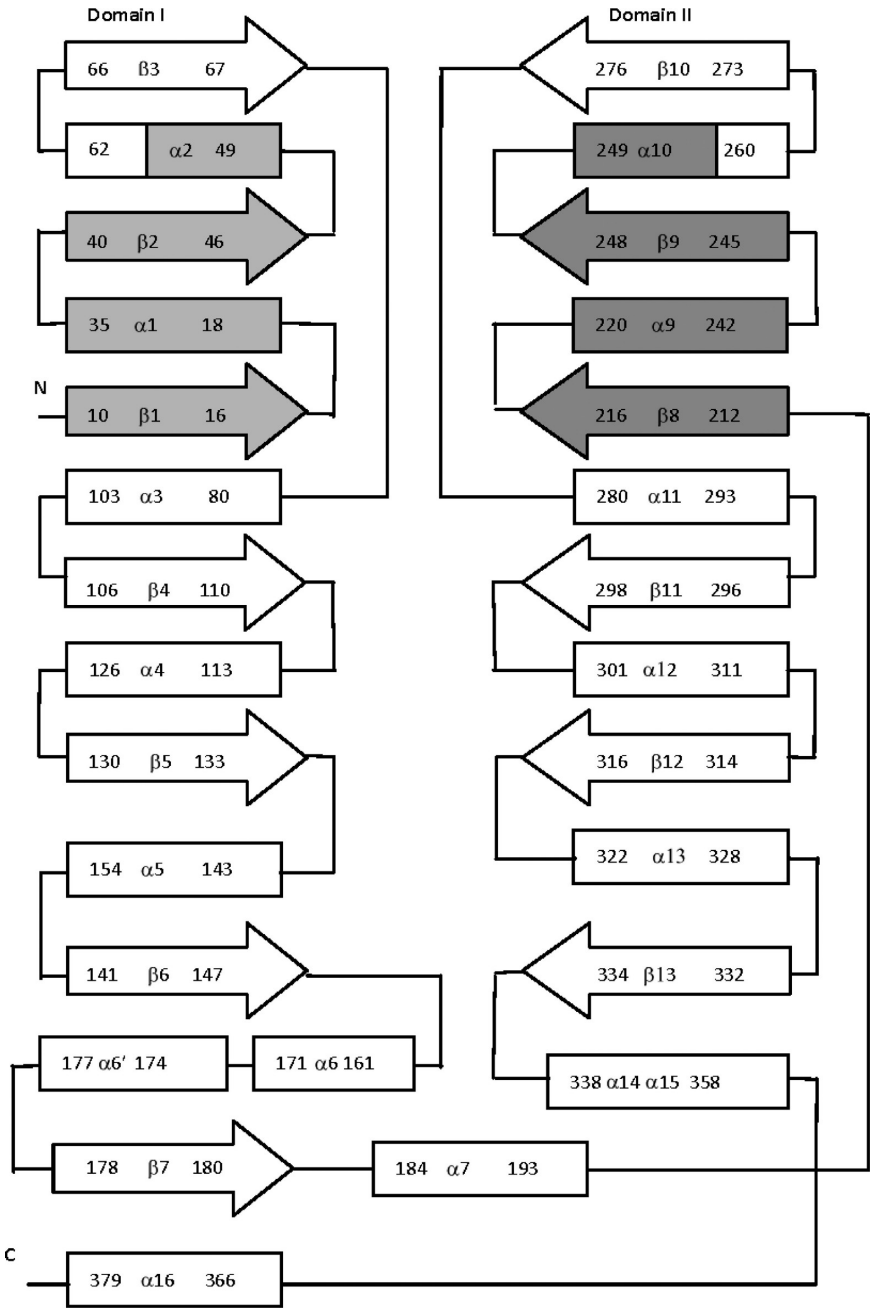

Figure 4. Secondary structure elements of the epimerase domain of the hGNE enzyme. Secondary structure elements, including domain, α-helix, and β-sheet structures,[11] of the hGNE1 isoform are shown. Elements deleted from domain I in the hGNE3, hGNE5, and hGNE8 isoforms (shaded in light gray) and in domain II in the hGNE5–hGNE8 isoforms (shaded in dark gray) are indicated. Numbers relate to hGNE1 amino acid numbering. N and C denote the N- and C-termini, respectively, of the GNE epimerase domain.

isoform, we did not further analyze hGNE4 secondary structure. In previous studies, structural elements and domains were assigned to the major hGNE1 isoform.[10,11] Here we align the secondary structure elements of the N- and C-terminal domains of the human GNE epimerase domain of all human GNE isoforms (Figures 3 and 4). There are two sites of differences among isoforms hGNE1–hGNE8 in the epimerase domain. The first site is at the N-terminus of (N-terminal) domain I, and the second site is at the N-terminus of (C-terminal) domain II (gray shaded regions in Figures 3, 4, and 5).

Modeling of the N-Terminal Extensions of hGNE2 and hGNE7. The hGNE2 and hGNE7 isoforms contain all of the hGNE1 isoform and, in addition, have a 31-residue N-terminal extension compared to hGNE1 (Figure 3A). Secondary structure prediction algorithms and our modeling of this 31-residue N-terminal extension indicated the possible presence of one or two additional α-helices (Figure 3B). An α-helical extension at the N-terminus of the nucleotide binding domains is present in some other proteins, like in *Squalus acanthias* muscle lactate dehydrogenase (LDH), where it is also involved in the formation of intersubunit contacts.[33] Extension of the Rossmann fold as an N-terminal extra helix is present in *Pseudomonas aeruginosa* UDP-*N*-acetylglucosamine 4-epimerase but not in *E. coli* UDP-galactose 4-epimerase.[34]

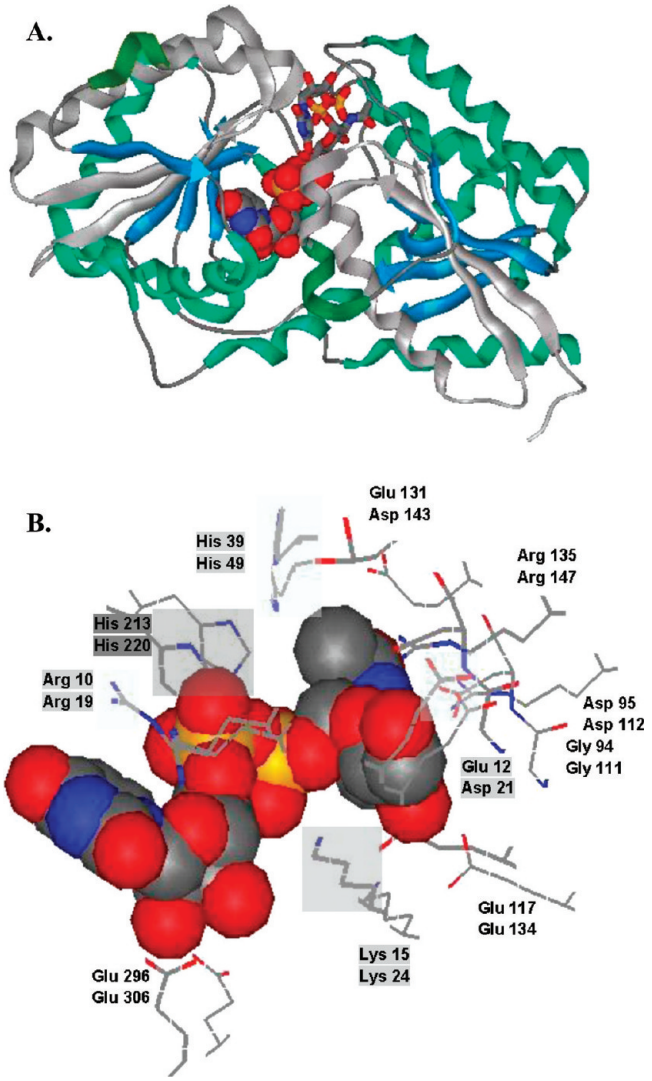

Figure 5. Tertiary structures of the major hGNE1 isoform and the active site of the GNE epimerase domain. (A) Model of the hGNE1 isoform. α-Helices (green) and β-sheets (blue) are shown. Fragments deleted from domain I (right) in hGNE3, hGNE5, or hGNE8 and fragments deleted from domain II (left) in hGNE5–hGNE8 are colored gray. In bacterial 2-epimerases, these deleted fragments contain an allosteric site where UDP-GlcNAc binds (spheres) and an active site where the UDP substrate binds (sticks). (B) Superposition of the three-dimensional structure of the *E. coli* 2-epimerase in complex with UDP-*N*-acetylglucosamine (PDB entry 1vgv) and the structure of the *H. sapiens* 2-epimerase domain of the hGNE1 isoform. Side chains of the active site residues (wire models), binding site residues of UDP-*N*-acetylglucosamine in *E. coli* 2-epimerase (top labels), and the corresponding residues in the human 2-epimerase domain of hGNE1 (bottom labels) are shown. Residues deleted from hGNE3, hGNE5, and hGNE8 are shaded in light gray (hGNE1 Arg19, Asp21, Lys24, and His49). The hGNE1 His220 residue, deleted from hGNE5–hGNE8, is colored dark gray. Red spheres represent oxygen, blue spheres nitrogen, gray spheres carbon, and yellow spheres phosphorus.

The hGNE2 and hGNE7 N-terminal extension is highly similar to α-helices in several other proteins, including the human serum and glucocorticoid-induced kinase 1 (SGK1) and *B. subtilis* putative transcriptional regulator YFHH (Table 2). SGK1 contains an intermolecular disulfide bond[35] in the region homologous to the hGNE2 and hGNE7 N-terminal extension. In SGK1, this region is predicted to come in close contact with an activation loop of the neighboring subunit and with its phosphorylation site.[35] Interestingly, a cysteine residue is present in the 31-amino acid N-terminal extension of hGNE2 and hGNE7 (at residue 12), as well as in the homologous SGK1 sequence and in several homologous histidine kinases (Figure 3B and Table 2). In addition, SGK1 (residues 175–240) harbors another region 25% homologous to GNE (residues 370–471 of hGNE1). This GNE region is located between the epimerase and kinase enzymatic domains and contains a cysteine at position 388. Cysteine residues C12 and C388 may be candidates for disulfide bonds; whether they are intermolecular (as in SGK1) or intramolecular (possibly between GNE regions) remains to be determined. However, as a cytosolic enzyme, disulfide bonds may be unlikely for GNE because of the reducing milieu. Whether the high degree of homology between SGK1 and GNE also provides data for similarities in structural or binding properties is a subject of future studies.

Modeling of the N-Terminal Extensions of hGNE3 and hGNE8. Compared to the major hGNE1 isoform, hGNE3 and hGNE8 contain a deletion of the first 55 N-terminal residues, including β1, α1, β2, and part of α2 (encoded by exon 3 in hGNE1). In addition, hGNE3 and hGNE8 contain a novel 50-residue N-terminal extension (encoded by exon 1). Secondary structure prediction algorithms and our modeling of the 50-residue N-terminal extension indicate the possible presence of alternating α-helices and β-strands (Figure 3B), which may serve as a replacement of the deleted fragment (β1, α1, β2, and part of α2) in the three-dimensional structure of the protein. In bacterial epimerase enzymes, the region homologous to the N-terminal portion of hGNE3 and hGNE8, including deleted β1, α1, β2, and part of α2 (Figures 3A and 4), contains an active site and an allosteric site. In the *B. anthracis* enzyme, this region is involved in contacts with the bacterial allosteric activator UDP-*N*-acetylglucosamine (mainly its phosphate and *N*-acetyl groups).

Alignment of the novel 50-residue fragment with the *A. orientalis* glycosyltransferase, also carrying a Rossmann fold [PDB entry 1rrv (Table 3)], suggests that it is likely that including the 50-residue extension may not change the overall fold of the protein. The N-terminal part of the 50-residue extension is less homologous to other proteins compared to the middle and C-terminal parts (Table 3). The middle part of the fragment is homologous to the *N*-acetyl-D-glucosamine binding region of α-1,2-mannosidase, which possesses an $(\alpha\alpha)_7$ fold and includes short β-strands (PDB entries 1hcu and 2r18). The C-terminal part of the fragment shows the highest level of similarity with *Saccharomyces cerevisiae* cytidine deaminase CDD1 (PDB entry 1r5t), which is involved in RNA editing activity.[36] Among the deaminase CDD1 active site residues, W79 and C86 align with the hGNE3 and hGNE8 N-terminal extension in the region conserved between the two enzymes (Table 3). Amino acid W79 (W80 and W86 in the homologous deaminases APOBEC1 and AID, respectively) forms a van der Waals contact with the cytosine edited by the deaminase activity, while C86 (C87 in AID) is involved in zinc coordination and nucleotide binding.[36] The tertiary structure of the deaminase CDD1 consists of a five-stranded β-sheet surrounded by three α-helices on both sides, similar to that of other deaminases and to the loops followed by a β-strand in the homologous N-terminal regions of hGNE3 and hGNE8. The *Mus musculus* deaminase (PDB entry 2fr5, 36% homologous to

Table 2. Amino Acid Similarities between the N-Terminal 31-Amino Acid Extension of the hGNE2 and hGNE7 Isoforms and Other Homologous Proteins

Protein/*source*/pdb code/	aa #[a]	Sequence alignment[b]
hGNE2 + hGNE7 extension	1-31	METYGYLQRESCFQGPHELYFKNLSKRNKQI
SGK1/ *H. sapiens* /2r5t/	183-202	ELFYHLQRERCFLEPRARFY
His kinase/ *A. avenae*/	198-213	FLQRERCFAGDASHEL
His kinase/ *P. carotovorum*/	194-219	DELERFLQRERCFVSDASHELRTPLA
His kinase/ *H. arsenicoxydans*/	193-216	AELQQFLARERFFTGDVSHELRTP
YFHH/ *B. subtilis*/1sf9/	8-31	SSGVDLGT----ENLYFQSNAMEKRYSQ
Leucyl-tRNA synthetase/ *T. thermophilus* /1obh /	703-733	LETSGVFQAEALEGKDRELYGKLHETLKKVT
Ubiquitin thioesterase/ *H. sapiens* /2zfy/	177-207	LLTSGYLQRESKFFEHFIEGGRTVKEFCQQE
Interleukin-5/ *H. sapiens* /1hul/	49-79	FQGIGTLESQTVQGGTVERLFKNLSLIKKYI
Cell division control protein/ *P. falciparum* /1v0p/	238-268	FTVYEPLPWESFLKGLDESGIDLLSKMLKLD
Ras-related C3 botulinum toxin/ *H. sapiens* /1ryf/	62-92	QEDYDRLRPLSYPQTVGETYGKDITSRGKDK
Cdc42-interacting protein/ *H. sapiens*/2efk/	71-101	QSFVQILQEVNDFAGQRELVAENLSVRVCLE
Hypothetical protein HP0495/ *H. pylori*/2h9z/	25-55	KDTSTLKELLETYQRPFKLEFKNTSKNAKFY
Ecor124i restriction enzyme/ *E. coli* /2w00/	192-222	NSLFKYLQLFVISNGTDTRYFANTTKRDKNS
ABC transporter/ *P. abyssi* /3bk7/	309-339	EFLQGYLKDENVRFRPYEIRFTKLSERVDVE

[a]Numbered range of amino acids. [b]Shaded, homologous fragments; double underlined, α-helices; underlined, β-sheets.

S. cerevisiae deaminase) binds the inhibitor tetrahydrouridine (PDB entry 2fr5)[37] in the proximity of the region homologous to the GNE 50-residue extension.

The deleted portion of the N-terminus of hGNE3 and hGNE8 compared to hGNE1 [β1, α1, β2, and part of α2 (Figure 3A)] contains several amino acids important for enzymatic function. Helix α1 (amino acids 18−35 of hGNE1) contains R19, D21, and K24 (Figures 3A and 4) corresponding to helix α1 (amino acids 9−26) and R10, E12, and K15 of the *E. coli* enzyme, which are located in the vicinity of the active site (K15 in *E. coli*) and are involved in stabilization of the structure (E12) and binding of the UDP portion of the substrate (R10). Of the amino acids located in the β2-α2 loop and helix α2 of hGNE1, which are deleted from hGNE3 and hGNE8 (Figure 3A), in *B. anthracis* 2-epimerase Q43, H44, and Q46 were found to compose an allosteric site and are conserved in bacterial enzymes. These residues, except the histidine, are not conserved in the human enzyme. The conserved histidine corresponds to H49 of the *Rattus rattus* and H49 of the *H. sapiens* 2-epimerase. This residue was shown to be directly involved in the epimerization process in rat GNE, which is 98% homologous to hGNE1. The H49A point mutation (erroneously indicated as H45A in ref 10) in the rat 2-epimerase resulted in the loss of GNE epimerase activity but not in kinase activity and did not appear to perturb the enzyme oligomeric state.[10]

Modeling of the Exon 5 Deletion in hGNE5−hGNE8.

The hGNE5−hGNE8 isoforms are derivatives of the hGNE1 isoform with deletion of a 53-amino acid fragment (encoded by exon 5) that includes β8, α9, β9, and part of α10 secondary structure elements (Figures 3A and 4). The deleted fragment contains a proposed catalytic residue, H220, which corresponds to H213 of the *E. coli* 2-epimerase (Figure 5B). Two amino acids from the deleted fragment form a bacterial allosteric site in the *B. anthracis* enzyme (R210 and H242) that are conserved in *V. cholera* and *E. coli* but not in *H. sapiens* 2-epimerase. Residue R210 of the *B. anthracis* 2-epimerase plays a role in anchoring UDP and UDP-GlcNAc and is conserved only in nonhydrolyzing enzymes. Residue H242 forms hydrogen bonds with the β-phosphate oxygen and a hydroxyl group of UDP-GlcNAc upon conformational change. It is assigned a role in the binding of UDP-GlcNAc at the allosteric site and stabilization of the UDP intermediate.

DISCUSSION

In this study, we explore GNE isoform expression in human tissues and compare structural differences between hGNE1 and six other human GNE isoforms by molecular modeling. In addition to the three previously described human GNE isoforms, database and PCR analysis yielded five additional hGNE isoforms, summarized in Figure 1. Because the commercially available GNE antibodies do not work well on Western blotting, we were unable to confirm expression of each transcript at the protein level. In our predictions below, we assumed each isoform transcript produces a protein.

Tissue analysis showed differential expression of the eight hGNE isoform-encoding transcripts. hGNE1 appeared to be the major isoform, with mRNA expression in all tissues tested. hGNE6 was the only other isoform whose mRNA was expressed in all tested tissues (although at low levels).

Table 3. Amino Acid Similarities between the N-Terminal 50-Amino Acid Extension of the hGNE3 and hGNE8 Isoforms and Other Homologous Proteins

Protein *Source* /pdb code/	aa #[a]	Sequence alignment[b]
hGNE3 + hGNE8 extension	1-50	MPIGDCSVAAKPRKQLLCSLFQTTLGYRARASGWKPMVICRGSHAFKDLI
Deaminase CDD1		
S. cerevisiae/1r5t/	77-89	SGWKCMVICGDS
M. musculus /2fr5/	81-91	D-FRAIAISSDL
Glycosyl transferase *A. orientalis* /1rrv/	346-394	IGVAHDGPTPTFESLSAALTTVLATRARAEAVAGMVLTDGAAAAADLV
Alpha-1,2-mannosidase		
T. reesei/1hcu/	88-103	TTNQGSSVFETNIRY
P. citrinum/ 2r18/	1113-1128	KTSDTVSLFETTIRY
Alkylsulfatase *P. aeruginosa* /2cg3/	496-506	LGYQAENAGWR
ATP12 ATPase *P. denitrificans* /2zd2/	1114-1124	RAQAEGWDPLI
Polycomb protein *H. sapiens* /2p0k/	112-142	PIGNCEKNG--------GMLQPPLGFRLNASSW-PMFLLK
Alpha-14 giardin *E. coli* /3chj/	80-92	KPRAQLLCELIR
Histidine-protein kinase *E. coli*/3iqt/	865-700	GSCGYSGVPRXKNLCQLIEQQLRSGTKEEDLEPELL
Galactoside O-acetyl-transferase *S. aureus* /3ftt/	42-58	ATNKRKELIDQLFQTT

[a]Numbered range of amino acids. [b]Shaded, homologous fragments; double underlined, α-helices; underlined, β-sheets.

hGNE6 likely has only kinase activity, because it lacks part of the epimerase functional domain (skipping of in-frame exon 5 compared to hGNE1). We identified four other h*GNE* transcripts (hGNE5, hGNE6, hGNE7, and hGNE8) that lacked exon 5 and, therefore, are predicted to display only kinase activity. The level of expression of hGNE5 was very low with conventional PCR (Figure 2A), and no h*GNE5*-specific TaqMan assay could be designed, limiting our further pursuit of hGNE5 expression. hGNE7 and hGNE8 followed a similar tissue distribution pattern and were expressed at low levels in selected human tissues (Figure 2 and Table 1). Interestingly, expression of hGNE2- and hGNE3-encoding transcripts followed the same tissue distribution pattern as that of hGNE7 and hGNE8, indicating that they may be regulated together. We did not detect hGNE4-encoding mRNA transcripts in tested tissues, and further analysis showed that this variant was submitted as a mutation identified in a DMRV patient (GenBank accession number EU093084), instead of a novel isoform. We list this variant because a GenBank accession number is ascribed to this isoform, listed in GenBank as variant 5, but we did not further analyze hGNE4 by molecular modeling.

Our cDNA analysis of a variety of mouse tissues identified transcripts encoding the two previously described mouse isoforms mGne1 and mGne2, which have high degrees of homology to hGNE1 and hGNE2 of 98.5 and 96.8%, respectively.[21] Orthologs of the other human isoforms do not appear to exist in mouse tissues, perhaps because of an evolutionary mechanism.

The highest h*GNE* mRNA expression levels occurred in the liver and placenta. Liver is the major organ of sialic synthesis and was shown to display high GNE enzymatic activity.[31] High-level hGNE expression in placenta may be related to an essential role of sialic acid during development.[31] The lowest level of hGNE mRNA expression was found in skeletal muscle, as previously described,[31] which may explain why skeletal muscle is the only affected tissue in HIBM/DMRV patients. A slight decrease in GNE enzymatic activities in HIBM/DMRV muscle may have a stronger effect on sialic acid supply in muscle than in other tissues that have higher natural GNE expression and enzyme activity levels. The effect of HIBM/DMRV patient mutations on hGNE isoform expression remains to be determined.

GNE epimerase and kinase enzymatic activities were reported for the hGNE1−hGNE3 isoforms.[22] Recombinantly expressed hGNE1 exhibited the highest epimerase activity (~1100 milliunits/mg) and existed in the tetrameric (full enzyme activity) and dimeric (kinase activity only) states. hGNE2 displayed an 80% reduction in epimerase activity compared to that of hGNE1 (~200 milliunits/mg) explained by its existence predominantly in the dimeric state. hGNE3 had no epimerase activity, likely because a part of the epimerase domain encoded by exon 3 is not expressed in this isoform. The oligomeric state of hGNE3 could not be determined because of low expression levels. hGNE1−hGNE3 all displayed high kinase activities (ranging from 2500 to 3500 milliunits/mg). Enzyme activities for isoforms hGNE5−hGNE8 are not known, but it is likely that they have no epimerase activity, because they lack exon 5, encoding part of the epimerase domain. In fact, our

modeling studies of these isoforms also predict diminished or absent epimerase activity. hGNE5−hGNE8 likely have residual kinase activity, because they express the kinase domain-encoding C-terminal exons. These results suggest that hGNE1 (with high epimerase activity) plays a major role in sialic acid production. The other human isoforms (with primarily kinase activity) may assist in the crucial regulation of cellular sialic acid levels.[22]

For molecular modeling, all considered human isoforms were analyzed in three groups. First, the 31-residue N-terminal extension compared to the hGNE1 isoform, occurring in hGNE2 and hGNE7, was analyzed. This extension produces α-helices that extend the Rossmann fold. Because similar extended Rossman folds N-terminal of the nucleotide binding domain are found in *S. acanthias* muscle lactate dehydrogenase, *P. aeruginosa* UDP-*N*-acetylglucosamine 4-epimerase, and other proteins, we assume the additional N-terminal fragments of hGNE2 and hGNE7 do not hinder the active sites of the GNE enzyme and will likely not eliminate epimerase activity. In fact, this was confirmed by enzyme activity measurements in recombinantly expressed hGNE2, which exhibited 80% epimerase activity and ManNAc kinase activity similar to that of hGNE1.[22] The 31-residue extension at the N-termini of hGNE2 and hGNE7 showed amino acid similarities with ATP-binding fragments of some kinases and helicases (Table 2). On the basis of homology to SGK1 and other kinases, the C12 residue in the 31-residue extension may be a candidate for disulfide bond formation. It was previously suggested that the 31-residue extension in GNE2 may play a regulatory role in fine-tuning sialic acid synthesis.[21,22]

Second, we considered the 55-residue N-terminal deletion and a novel 50-residue extension in the hGNE3 and hGNE8 isoforms. Interestingly, the size and secondary structure [alternating α-helices and β-strands (Figure 3)] of the deleted and extension fragments are similar, indicating that the extension may serve as a replacement for the deletion. In addition, the novel 50-residue extension is similar to other proteins containing the Rossmann fold such as deaminases, glycosyltransferases, α-1,2-mannosidase, ATPase, and guardian (Table 3). These findings indicate that the N-terminal modification of hGNE3 and hGNE8 may not affect the overall fold of the protein, compared to that of hGNE1. However, the epimerase function of the hGNE3 and hGNE8 isoforms is predicted to be weakened or absent, because the deleted 55-residue fragment contains several amino acids important for enzymatic function, including substrate binding. In homologous bacterial epimerase enzymes, this region is part of an active and allosteric site. In addition, it was shown that deletion of the 39 N-terminal amino acids of hGNE1 leads to the complete loss of epimerase activity with 22% of the kinase activity retained.[32] Indeed, measurements of the activity of the recombinant hGNE3 enzyme confirmed the loss of epimerase enzymatic activity and the retention of ManNAc kinase activity, likely because of the presence of the unaffected kinase domain.[21,22]

Lastly, in addition to an N-terminal modification, a 53-residue deletion occurring in hGNE5−hGNE8 was considered. The deleted region contains a predicted catalytic residue and is assigned a role in the binding of UDP-GlcNAc and stabilization of the UDP intermediate (displayed in Figure 5A). Deletion of this fragment likely results in abolished epimerase activity, while ManNAc kinase activity may remain present. No enzymatic studies have been performed for these isoforms. The hGNE5 isoform contains the 53-residue deletion mentioned above (encoded by exon 5) as well as a 110-residue N-terminal deletion (and no extension) compared to hGNE1. Therefore, hGNE5 is also predicted to have abolished epimerase activity with residual kinase activity, which remains to be confirmed by enzymatic activity measurements.

We previously established that the major GNE1 isoform consists of seven-stranded parallel β-sheets sandwiched between a total of seven α-helices in the N-terminal domain and a six-stranded β-sheet surrounded by a total of seven α-helices in the C-terminal domain.[11] The epimerase-encoding region of GNE consists of two domains, domain I (N-terminal) and domain II (C-terminal) (Figure 4). These two domains show structural similarities, and both have a topology similar to the Rossman nucleotide binding fold. Interestingly, the two major deleted fragments in the hGNE isoforms, one 55-residue deletion at the N-terminus of domain I in the hGNE3 and hGNE8 isoforms and the other a 53-residue deletion at the N-terminus of domain II in the hGNE5−hGNE8 isoforms (Figures 2 and 3), also show structural similarities between each other. Both deleted fragments consist of βαβα secondary structure elements at their N-termini, and both contain similarly located conserved active site residue(s) and non-conserved bacterial allosteric site amino acid residues. It is possible that the evolution of the different hGNE isoforms illustrates a process of the elimination of the bacterial allosteric site from the enzyme, as well as further evolution of the mammalian bifunctional enzyme from two separate bacterial epimerase and kinase enzymes.

Evolution displays several mechanisms by which the number of cellular functions can be increased, without increasing the number of genes.[38] These include expression of multiple mRNAs from one gene (by alternative mRNA transcription or alternative splicing), multiple translation products from one gene (by initiation of translation from alternative in-frame start codons), tissue-specific mRNA or protein expression, targeting of protein to different cellular compartments, post-translational protein modification (through phosphorylation, glyscosylation, etc.), and oligomer formation, among others. It appears as if the *GNE* gene is an excellent example of being subjected to some of the mechanisms mentioned above. First, the *GNE* gene displays an increased number of mRNA transcripts through evolution; while the mouse *Gne* gene has only two mRNA transcripts, the human *GNE* gene produces at least seven different transcripts (formed by alternative splicing, alternative transcription, or both). Second, *GNE* mRNA transcripts are tissue-specifically expressed, possibly because of tissue-specific demands for sialylation or other regulatory processes independent of sialic acid production, such as sialyltransferase expression, ganglioside production, and modulation of proliferation and apoptosis.[39] Third, the different hGNE isoforms (if translated) may be differently localized within the cell. hGNE1 can be localized to the nucleus, cytoplasm, or the Golgi region, perhaps targeted by a putative leucine rich nuclear export signal, located within amino acids 121−140 of hGNE1.[40] This region is highly conserved and is not deleted or modified in any of the other human isoforms. Fourth, hGNE has several potential phosphorylation sites that may affect function.[41] Some predicted phosphorylation sites (by NetPhos 2.0) are deleted from (Thr34, Tyr22, and Tyr54 of hGNE1 are deleted from hGNE3, hGNE5, and hGNE8) or added to (Ser11 and Tyr4 of hGNE2 and hGNE7 are not present in hGNE1) the different hGNE isoforms compared to hGNE1. Finally, GNE exists in two major oligomeric states, tetramers and dimers, which

engage in dynamic interplay with monomers and higher aggregates. As a monomer, GNE has no enzymatic activity; its dimer exhibits only ManNAc kinase activity, and the tetrameric state displays both UDP-GlcNAc 2-epimerase and ManNAc kinase activities.[42] In addition, the fully functional tetrameric state of GNE is stabilized by ligands of the epimerase domain, UDP-GlcNAc and CMP-Neu5Ac. Our molecular modeling studies may contribute to predictions of the involvement of isoforms in oligomer formation and enzyme activity of oligomeric complexes.

In summary, our human GNE isoform studies revealed that hGNE1 exists as a ubiquitously expressed, major isoform, while hGNE2−hGNE8 isoforms are differentially expressed and may act as tissue-specific regulators of sialylation. Genetic analysis of the novel coding regions of h*GNE* exons 1−3 is warranted in patients with HIBM/DMRV, especially those in which only one *GNE* mutation could be identified. These expression and structural prediction data may contribute to elucidation of the complex functional and regulatory mechanisms of GNE, as well as to further elucidation of the pathology and treatment strategies of the human GNE-opathies sialuria and HIBM/DMRV, as well as of other disorders of hyposialylation.

■ ASSOCIATED CONTENT

Ⓢ Supporting Information

Primer sequences for PCR amplification of the human *GNE* transcripts (*hGNE*) (Table S1) and TaqMan primer and probe sequences for qPCR for determining the levels of expression of *hGNE* transcripts (Table S2). This material is available free of charge via the Internet at http://pubs.acs.org.

■ AUTHOR INFORMATION

Corresponding Author

*NHGRI, NIH, 10 Center Dr., Building 10, Room 10C103, Bethesda, MD 20892-1851. Phone: (301) 402-2797. Fax: (301) 480-7825. E-mail: mhuizing@mail.nih.gov.

Funding

This study was supported by the Intramural Research Program of the National Human Genome Research Institute, National Institutes of Health (T.Y., K.J., C.C., K.P., W.A.G., and M.H.) and Research Funds of The School of Theoretical Modeling (T.C. and N.K.).

■ ACKNOWLEDGMENTS

We greatly appreciate the expert laboratory work of Katherine Berger and Adrian Astiz-Martinez. This work was performed in partial fulfillment of the requirements for a Ph.D. degree of T.Y. in the Sackler Faculty of Medicine of Tel Aviv University.

■ ABBREVIATIONS

ASKHA, acetate and sugar kinase/Hsp70/actin; B2M, β2-microglobulin; BLAST, Basic Local Alignment Search Tool; CDD1, cytidine deaminase 1; CDM, Consensus Data Mining; CMP, cytidine monophosphate; DMRV, distal myopathy with rimmed vacuoles; FDM, Fragment Database Mining; GAPDH, glyceraldehyde-3-phosphate dehydrogenase; GNE, uridine diphospho-*N*-acetylglucosamine (UDP-GlcNAc) 2-epimerase/*N*-acetylmannosamine (ManNAc) kinase; GOR, Garnier−Osguthorpe−Robson; HIBM, hereditary inclusion body myopathy; LDH, lactate dehydrogenase; MDH, malate dehydrogenase; NCBI, National Center for Biotechnology Information; Neu5Ac, *N*-acetylneuraminic acid; OMIM, Online Mendelian Inheritance in Man; qPCR, quantitative real-time polymerase chain reaction; PDB, Protein Data Bank; PSIPRED, Protein Structure Initiative Prediction; SGK1, glucocorticoid-induced kinase 1; *A. avenae*, *Acidovorax avenae*; *A. orientalis*, *Amycolatopsis orientalis*; *H. arsenicoxydans*, *Herminiimonas arsenicoxydans*; *H. pylori*, *Helicobacter pylori*; *P. abyssi*, *Pyrococcus abyssi*; *P. carotovorum*, *Pectobacterium carotovorum*; *P. citrinum*, *Penicillium citrinum*; *P. denitrificans*, *Paracoccus denitrificans*; *P. falciparum*, *Plasmodium falciparum*; *S. aureus*, *Staphylococcus aureus*; *T. thermophilus*, *Thermus thermophilus*; *T. reesei*, *Trichoderma reesei*.

■ REFERENCES

(1) Hinderlich, S., Stasche, R., Zeitler, R., and Reutter, W. (1997) A bifunctional enzyme catalyzes the first two steps in N-acetylneuraminic acid biosynthesis of rat liver. Purification and characterization of UDP-N-acetylglucosamine 2-epimerase/N-acetylmannosamine kinase. *J. Biol. Chem. 272*, 24313−24318.

(2) Eisenberg, I., Avidan, N., Potikha, T., Hochner, H., Chen, M., Olender, T., Barash, M., Shemesh, M., Sadeh, M., Grabov-Nardini, G., Shmilevich, I., Friedmann, A., Karpati, G., Bradley, W. G., Baumbach, L., Lancet, D., Asher, E. B., Beckmann, J. S., Argov, Z., and Mitrani-Rosenbaum, S. (2001) The UDP-N-acetylglucosamine 2-epimerase/N-acetylmannosamine kinase gene is mutated in recessive hereditary inclusion body myopathy. *Nat. Genet. 29*, 83−87.

(3) Chen, X., and Varki, A. (2010) Advances in the biology and chemistry of sialic acids. *ACS Chem. Biol. 5*, 163−176.

(4) Varki, N. M., and Varki, A. (2007) Diversity in cell surface sialic acid presentations: Implications for biology and disease. *Lab. Invest. 87*, 851−857.

(5) Kornfeld, S., Kornfeld, R., Neufeld, E. F., and O'Brien, P. J. (1964) The Feedback Control of Sugar Nucleotide Biosynthesis in Liver. *Proc. Natl. Acad. Sci. U.S.A. 52*, 371−379.

(6) Seppala, R., Lehto, V. P., and Gahl, W. A. (1999) Mutations in the human UDP-N-acetylglucosamine 2-epimerase gene define the disease sialuria and the allosteric site of the enzyme. *Am. J. Hum. Genet. 64*, 1563−1569.

(7) Leroy, J. G., Seppala, R., Huizing, M., Dacremont, G., De Simpel, H., Van Coster, R. N., Orvisky, E., Krasnewich, D. M., and Gahl, W. A. (2001) Dominant inheritance of sialuria, an inborn error of feedback inhibition. *Am. J. Hum. Genet. 68*, 1419−1427.

(8) Huizing, M., and Krasnewich, D. M. (2009) Hereditary inclusion body myopathy: A decade of progress. *Biochim. Biophys. Acta 1792*, 881−887.

(9) Noguchi, S., Keira, Y., Murayama, K., Ogawa, M., Fujita, M., Kawahara, G., Oya, Y., Imazawa, M., Goto, Y., Hayashi, Y. K., Nonaka, I., and Nishino, I. (2004) Reduction of UDP-N-acetylglucosamine 2-epimerase/N-acetylmannosamine kinase activity and sialylation in distal myopathy with rimmed vacuoles. *J. Biol. Chem. 279*, 11402−11407.

(10) Effertz, K., Hinderlich, S., and Reutter, W. (1999) Selective loss of either the epimerase or kinase activity of UDP-N-acetylglucosamine 2-epimerase/N-acetylmannosamine kinase due to site-directed mutagenesis based on sequence alignments. *J. Biol. Chem. 274*, 28771−28778.

(11) Kurochkina, N., Yardeni, T., and Huizing, M. (2010) Molecular modeling of the bifunctional enzyme UDP-GlcNAc 2-epimerase/ManNAc kinase and predictions of structural effects of mutations associated with HIBM and sialuria. *Glycobiology 20*, 322−337.

(12) Velloso, L. M., Bhaskaran, S. S., Schuch, R., Fischetti, V. A., and Stebbins, C. E. (2008) A structural basis for the allosteric regulation of non-hydrolysing UDP-GlcNAc 2-epimerases. *EMBO Rep. 9*, 199−205.

(13) Rao, S. T., and Rossmann, M. G. (1973) Comparison of super-secondary structures in proteins. *J. Mol. Biol. 76*, 241−256.

(14) Ha, S., Walker, D., Shi, Y., and Walker, S. (2000) The 1.9 Å crystal structure of *Escherichia coli* MurG, a membrane-associated glycosyltransferase involved in peptidoglycan biosynthesis. *Protein Sci. 9*, 1045−1052.

(15) Campbell, R. E., Mosimann, S. C., Tanner, M. E., and Strynadka, N. C. (2000) The structure of UDP-N-acetylglucosamine 2-epimerase reveals homology to phosphoglycosyl transferases. *Biochemistry 39*, 14993−15001.
(16) Tong, Y., Tempel, W., Nedyalkova, L., Mackenzie, F., and Park, H. W. (2009) Crystal structure of the N-acetylmannosamine kinase domain of GNE. *PLoS One 4*, e7165.
(17) Nishimasu, H., Fushinobu, S., Shoun, H., and Wakagi, T. (2007) Crystal structures of an ATP-dependent hexokinase with broad substrate specificity from the hyperthermophilic archaeon *Sulfolobus tokodaii*. *J. Biol. Chem. 282*, 9923−9931.
(18) Bork, P., Sander, C., and Valencia, A. (1992) An ATPase domain common to prokaryotic cell cycle proteins, sugar kinases, actin, and hsp70 heat shock proteins. *Proc. Natl. Acad. Sci. U.S.A. 89*, 7290−7294.
(19) Mukai, T., Kawai, S., Mori, S., Mikami, B., and Murata, K. (2004) Crystal structure of bacterial inorganic polyphosphate/ATP-glucomannokinase. Insights into kinase evolution. *J. Biol. Chem. 279*, 50591−50600.
(20) Watts, G. D., Thorne, M., Kovach, M. J., Pestronk, A., and Kimonis, V. E. (2003) Clinical and genetic heterogeneity in chromosome 9p associated hereditary inclusion body myopathy: Exclusion of GNE and three other candidate genes. *Neuromuscular Disord. 13*, 559−567.
(21) Reinke, S. O., and Hinderlich, S. (2007) Prediction of three different isoforms of the human UDP-N-acetylglucosamine 2-epimerase/N-acetylmannosamine kinase. *FEBS Lett. 581*, 3327−3331.
(22) Reinke, S. O., Eidenschink, C., Jay, C. M., and Hinderlich, S. (2009) Biochemical characterization of human and murine isoforms of UDP-N-acetylglucosamine 2-epimerase/N-acetylmannosamine kinase (GNE). *Glycoconjugate J. 26*, 415−422.
(23) Bernstein, F. C., Koetzle, T. F., Williams, G. J., Meyer, E. F. Jr., Brice, M. D., Rodgers, J. R., Kennard, O., Shimanouchi, T., and Tasumi, M. (1977) The Protein Data Bank: A computer-based archival file for macromolecular structures. *J. Mol. Biol. 112*, 535−542.
(24) Schmittgen, T. D., and Livak, K. J. (2008) Analyzing real-time PCR data by the comparative C(T) method. *Nat. Protoc. 3*, 1101−1108.
(25) Garnier, J., Osguthorpe, D. J., and Robson, B. (1978) Analysis of the accuracy and implications of simple methods for predicting the secondary structure of globular proteins. *J. Mol. Biol. 120*, 97−120.
(26) Kloczkowski, A., Ting, K. L., Jernigan, R. L., and Garnier, J. (2002) Combining the GOR V algorithm with evolutionary information for protein secondary structure prediction from amino acid sequence. *Proteins 49*, 154−166.
(27) Cheng, H., Sen, T. Z., Kloczkowski, A., Margaritis, D., and Jernigan, R. L. (2005) Prediction of protein secondary structure by mining structural fragment database. *Polymer 46*, 4314−4321.
(28) Sen, T. Z., Cheng, H., Kloczkowski, A., and Jernigan, R. L. (2006) A Consensus Data Mining secondary structure prediction by combining GOR V and Fragment Database Mining. *Protein Sci. 15*, 2499−2506.
(29) Bryson, K., McGuffin, L. J., Marsden, R. L., Ward, J. J., Sodhi, J. S., and Jones, D. T. (2005) Protein structure prediction servers at University College London. *Nucleic Acids Res. 33*, W36−W38.
(30) Eisenberg, I., Grabov-Nardini, G., Hochner, H., Korner, M., Sadeh, M., Bertorini, T., Bushby, K., Castellan, C., Felice, K., Mendell, J., Merlini, L., Shilling, C., Wirguin, I., Argov, Z., and Mitrani-Rosenbaum, S. (2003) Mutations spectrum of GNE in hereditary inclusion body myopathy sparing the quadriceps. *Hum. Mutat. 21*, 99.
(31) Lucka, L., Krause, M., Danker, K., Reutter, W., and Horstkorte, R. (1999) Primary structure and expression analysis of human UDP-N-acetyl-glucosamine-2-epimerase/N-acetylmannosamine kinase, the bifunctional enzyme in neuraminic acid biosynthesis. *FEBS Lett. 454*, 341−344.
(32) Blume, A., Weidemann, W., Stelzl, U., Wanker, E. E., Lucka, L., Donner, P., Reutter, W., Horstkorte, R., and Hinderlich, S. (2004) Domain-specific characteristics of the bifunctional key enzyme of sialic acid biosynthesis, UDP-N-acetylglucosamine 2-epimerase/N-acetylmannosamine kinase. *Biochem. J. 384*, 599−607.
(33) Abad-Zapatero, C., Griffith, J. P., Sussman, J. L., and Rossmann, M. G. (1987) Refined crystal structure of dogfish M4 apo-lactate dehydrogenase. *J. Mol. Biol. 198*, 445−467.
(34) Ishiyama, N., Creuzenet, C., Lam, J. S., and Berghuis, A. M. (2004) Crystal structure of WbpP, a genuine UDP-N-acetylglucosamine 4-epimerase from *Pseudomonas aeruginosa*: Substrate specificity in UDP-hexose 4-epimerases. *J. Biol. Chem. 279*, 22635−22642.
(35) Zhao, B., Lehr, R., Smallwood, A. M., Ho, T. F., Maley, K., Randall, T., Head, M. S., Koretke, K. K., and Schnackenberg, C. G. (2007) Crystal structure of the kinase domain of serum and glucocorticoid-regulated kinase 1 in complex with AMP PNP. *Protein Sci. 16*, 2761−2769.
(36) Xie, K., Sowden, M. P., Dance, G. S., Torelli, A. T., Smith, H. C., and Wedekind, J. E. (2004) The structure of a yeast RNA-editing deaminase provides insight into the fold and function of activation-induced deaminase and APOBEC-1. *Proc. Natl. Acad. Sci. U.S.A. 101*, 8114−8119.
(37) Teh, A. H., Kimura, M., Yamamoto, M., Tanaka, N., Yamaguchi, I., and Kumasaka, T. (2006) The 1.48 Å resolution crystal structure of the homotetrameric cytidine deaminase from mouse. *Biochemistry 45*, 7825−7833.
(38) Yogev, O., and Pines, O. (2011) Dual targeting of mitochondrial proteins: Mechanism, regulation and function. *Biochim. Biophys. Acta 1808*, 1012−1020.
(39) Wang, Z., Sun, Z., Li, A. V., and Yarema, K. J. (2006) Roles for UDP-GlcNAc 2-epimerase/ManNAc 6-kinase outside of sialic acid biosynthesis: Modulation of sialyltransferase and BiP expression, GM3 and GD3 biosynthesis, proliferation, and apoptosis, and ERK1/2 phosphorylation. *J. Biol. Chem. 281*, 27016−27028.
(40) Krause, S., Hinderlich, S., Amsili, S., Horstkorte, R., Wiendl, H., Argov, Z., Mitrani-Rosenbaum, S., and Lochmuller, H. (2005) Localization of UDP-GlcNAc 2-epimerase/ManAc kinase (GNE) in the Golgi complex and the nucleus of mammalian cells. *Exp. Cell Res. 304*, 365−379.
(41) Horstkorte, R., Nohring, S., Danker, K., Effertz, K., Reutter, W., and Lucka, L. (2000) Protein kinase C phosphorylates and regulates UDP-N-acetylglucosamine-2-epimerase/N-acetylmannosamine kinase. *FEBS Lett. 470*, 315−318.
(42) Ghaderi, D., Strauss, H. M., Reinke, S., Cirak, S., Reutter, W., Lucka, L., and Hinderlich, S. (2007) Evidence for dynamic interplay of different oligomeric states of UDP-N-acetylglucosamine 2-epimerase/N-acetylmannosamine kinase by biophysical methods. *J. Mol. Biol. 369*, 746−758.